

Stereolithographic biomodelling to create tangible hard copies of the ethmoidal labyrinth air cells based on the visible human project

S. Kapakin

Department of Anatomy, Faculty of Medicine, Atatürk University, Erzurum, Turkey

[Received 6 December 2010; Accepted 13 January 2011]

Rapid prototyping (RP), or stereolithography, is a new clinical application area, which is used to obtain accurate three-dimensional physical replicas of complex anatomical structures. The aim of this study was to create tangible hard copies of the ethmoidal labyrinth air cells (ELACs) with stereolithographic biomodelling. The visible human dataset (VHD) was used as the input imaging data. The Surfdriver software package was applied to these images to reconstruct the ELACs as three-dimensional DXF (data exchange file) models. These models were post-processed in 3D-Doctor software for virtual reality modelling language (VRML) and STL (Standard Triangulation Language) formats. Stereolithographic replicas were manufactured in a rapid prototyping machine by using the STL format. The total number of ELACs was 21. The dimensions of the ELACs on the right and left sides were $52.91 \times 13.00 \times 28.68$ mm and $53.79 \times 12.42 \times 28.55$ mm, respectively. The total volume of the ELACs was 4771.1003 mm³. The mean ELAC distance was 27.29 mm from the nasion and 71.09 mm from the calotte topologically. In conclusion, the combination of Surfdriver and 3D-Doctor could be effectively used for manufacturing 3D solid models from serial sections of anatomical structures. Stereolithographic anatomical models provide an innovative and complementary tool for students, researchers, and surgeons to apprehend these anatomical structures tangibly. The outcomes of these attempts can provide benefits in terms of the visualization, perception, and interpretation of the structures in anatomy teaching and prior to surgical interventions. (Folia Morphol 2011; 70, 1: 33–40)

Key words: ethmoidal labyrinth air cells, 3D reconstruction, stereolithography, VRML, anaglyph, photorealistic imaging, topology

INTRODUCTION

Computer and digital radiographic technology and techniques have significantly expanded the possibilities for accurate, quantitative, and noninvasive visualization and measurement of intracorporeal morphology and function during the last four decades. Three-

-dimensional (3D) imaging and visualization methods are emerging as the method of choice in many clinical examinations, replacing some previously routine procedures, and significantly complementing others [31].

Three-dimensional imaging and visualization efforts have been primarily directed toward the dis-

play and visualization of the contained information. There is also a need for modelling and analysis of the relevant information obtained from images [7]. Hence, tomographic techniques such as X-ray computed tomography (CT) and magnetic resonance imaging (MRI) could be coupled with computer graphics to create realistic 3D digital models of scanned structures. Stereolithography uses digital model data to produce physical models, thus offering a unique way of displaying and remodelling individual patient anatomy [42].

To our knowledge, due to the separate and small parts of ethmoidal labyrinth air cells (ELACs), stereolithographic models of ELACs have not been developed. The aims of this study were to create 3D computer-aided design (CAD) models and tangible hard copies (stereolithographic replicas) of ELACs and offer the possibility of 3D visualization using different techniques.

MATERIAL AND METHODS

Data source

We used imaging data from the visible human dataset, which is part of the visible human project (VHP), initiated by the National Library of Medicine (NLM). The visible human data exists in different modalities: CT, MRI, and anatomical cryosections [1]. In this study, anatomical cryosections were used since they were high-resolution cross-sectional coloured images and provided better anatomical information than the other modalities [7].

Cryosectional image features

To obtain the cryosection images, the cadaver was first frozen solid inside a large block of blue gel. Then, one-millimetre thick slices were successively cut away from an axial cross-section (planar cut perpendicular to the longitudinal axis of the body), and digital colour images were taken of each newly exposed cross-section. A total of 1878 cryosection images were taken, spanning the body from head to toe. Each was in 24-bit colour and had a resolution of 1748 x 966 pixels [35].

Software platforms

Five software programs were used in this study: Adobe Photoshop CS for image enhancement; SURFdriver 3.5 for segmentation, registration, surfacing, and quantitative analysis; 3D-Doctor for simulation, animation, and rapid prototyping applications; Cinema 4D for photorealistic and topologic modelling;

and Cortona VRML 6.0 for viewing the scenes on the Internet.

Creation of the computer-aided design model of the ethmoidal labyrinth air cells

The spatial extent of the ELACs was identified to provide surface models from serial cryosections using the Surfdriver software. Surface models represent the geometric structure, which is helpful for fabricating prostheses, inspecting occluded joints, pre-operative simulation, and post-operative analysis [30]. Moreover, these models are necessary for simulation/animation and real-time rendering [7]. The model preparation can be divided into registration, segmentation, and surface reconstruction stages. Prior to the model preparation, cryosectional images from the Surfdriver software's visible human CD were taken and converted to Microsoft Windows Device Independent Bitmap (BMP) file format. Sections were registered to each other to get an initial ground truth after substantiating their compatibility using both manual and automatic tools as well as visual inspection [8]. Segmentation is a prerequisite of reconstruction that can be based on a set of serial sections obtained by physical sectioning (cryosectioning) or by virtual sectioning from CT or MRI. The segmentation process was based on the osseous contours, i.e. the osseous outlines minus the mucosa in our study. Segmentation covers identification and delineation of the organ in the cross-sectional images. The organ can be defined as the surface of an empty shell. In the 2D sectional image, the surface approach is to determine the boundary of the organ as a contour, section by section. A set of points on the surface ("nodes") and information about how these nodes are linked to their neighbours ("facet descriptors") are used to define the organ in order to reconstruct an organ surface. Once the organ was interpreted and labelled on the different cross-sections as contours, 3D reconstruction was achieved by joining the contours of all the pertinent slices using the Surfdriver software to obtain a 3D surface model (Figs. 1A, B) [12]. In this study, after a 3D surface model of the ELACs was generated, the model was converted to the DXF file format to process the model further for 3D-Doctor and Cinema 4D software.

Creation of the photorealistic and topological models of the ethmoidal labyrinth air cells

The CAD model in DXF file format was transferred into Cinema 4D to be used by the Advanced Render

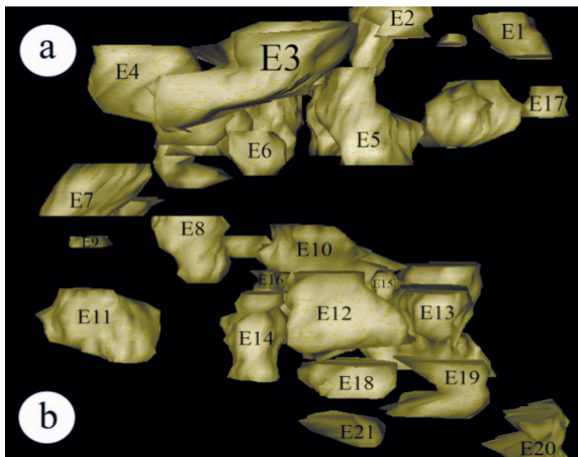


Figure 1. Lateral views of the ethmoidal labyrinth air cells, (A) right and (B) left. Surface modelling first involves identification of the region of desired tissue in the volume and then construction of a description of this region as a surface.

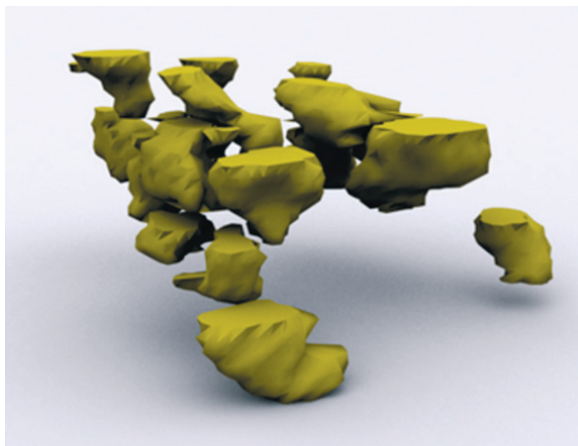


Figure 2. Photorealistic postero-lateral views of the ethmoidal labyrinth air cells using Cinema 4D software. All the anatomical details belonging to the ethmoidal labyrinth air cells can be seen with high sensitivity.

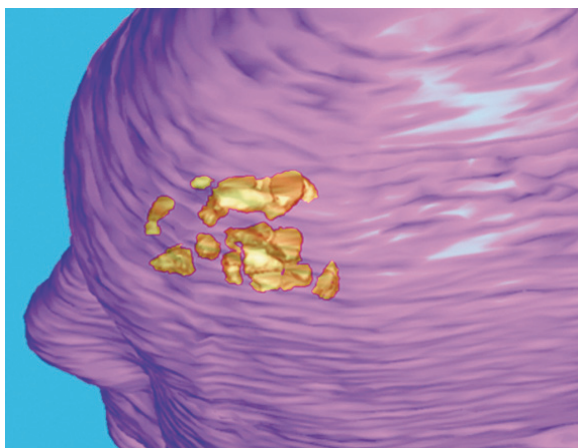


Figure 3. The topographical position of the ethmoidal labyrinth air cells in the cranium. The ethmoidal labyrinth air cells were reconstructed from the cryosections, thus exhibiting the original organ texture.

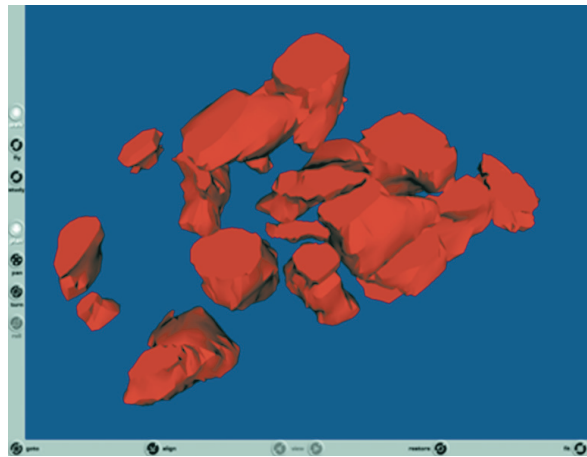


Figure 4. A view of the ethmoidal labyrinth air cells using virtual reality modelling language model.



Figure 5. An image of a three-dimensional solid biomodel of all the Ethmoidal Labyrinth Air Cells together created with the stereolithography technique.

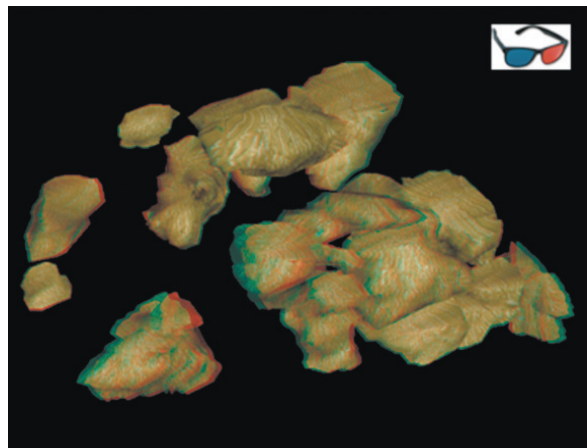


Figure 6. An anaglyphic image of reconstructed ethmoidal labyrinth air cells with Adobe Photoshop CS. A stereo image that requires anaglyphic glasses with blue glass in the right lens and red glass in the left lens for 3D viewing and depth perception. Three-dimensional view perception could not be sensed if stereoblindness is present.

Module. The results can be spectacularly realistic, but incredibly time consuming (Fig. 2) [16]. Topology in our context was defined as a 3D connectivity graph of anatomical structures for given body parts. Topological information thus provides inter-relationships among structures (Fig. 3) [7].

The CAD model in DXF file format could also be saved in VRML format for display on the web (Fig. 4). The application of the VRML as a portable file format for describing three-dimensional views of anatomical structures has enabled students, researchers, and surgeons to share anatomical models on the web [38].

Creation of the stereolithographic model of the ethmoidal labyrinth air cells

The first step in rapid prototyping (RP) is to develop a CAD model in DXF file format using Surfdriver software. The volume of this model is then meshed or broken into small elements. Each element is described by the (x, y, z) coordinates of the end points and the outward normal. The file containing all information about the mesh elements is known as the STL file [2]. The CAD model in DXF file format could be converted into the STL file format using 3D-Doctor software, which is readable by most prototyping machines. The STL file is exported to the software that comes with the rapid prototyping machine [2]. Once the STL file is generated from the original CAD data, the next step is to slice the object horizontally to create a slice file (SLI). The files are then merged into a final build file. The sliced model is exported to the rapid prototyping machine. The RP process is additive. That is, it builds the parts up in layers of material from the bottom. Each layer is automatically bonded to the layer below, and the process is repeated until the part is built [19]. Finally, the stereolithograms of the ELACs are obtained (Fig. 5).

Creation of the anaglyph form of the ethmoidal labyrinth air cells

Anaglyphic stereograms (anaglyphs) are stereo pairs of 3D images in which each image is shown using a different colour. Anaglyphic images are specific images viewed using special anaglyph glasses that allow only one part of the stereo pair to be visualized by each eye and its depth is perceived with a cerebral organization. The standard approach is to obtain two images of the object that differ in their effective viewing angle by 8–10°. The two images are overlapped and then viewed using red/blue or red/green glasses, depending on the colours used

[5, 29]. In our case, left and right colour stereo pairs of the ELAC images were combined to create anaglyphs by Adobe Photoshop (Fig. 6). First, both images were transformed to greyscale images, and they were then transformed back to RGB (red, green, blue) images. Thereafter, the red component of the left stereo pair was copied to the red component of the right stereo pair, extinguishing the red component of the right image. A duo-chromatic digital image was created that could be printed using photographic-quality printers [5].

RESULTS

A model of the ELACs within the head of the male Visible Human was built. The ELACs were numbered from E1 to E21 in order of their appearance in the cryosections (Figs. 1A, B).

Morphometry and topology

With the morphometric evaluation of the ELAC reconstructions, on the right side, the ELACs dimensions were 52.91 mm longitudinally, 13.00 mm laterally, and 28.68 mm vertically. On the left side, the ELACs dimensions were 53.79 mm longitudinally, 12.42 mm laterally, and 28.55 mm vertically. The total number of ELACs was 21; 14 on the left side and 7 on the right side. The total volume of the ELACs was 4771.1003 mm³ (Table 1). The largest cell was located in the middle part of the ethmoidal labyrinth. Mean distance was 27.29 mm from the root of the nose (nasion) and 71.09 mm from the skullcap (calotte), topologically.

Methodology

The Surfdriver and 3D-Doctor pair can be reliably and reproducibly used for manufacturing 3D solid models from the serial sections of anatomical structures in different modalities such as CT, MRI, and anatomical cryosections. The combination of Surfdriver and 3D-Doctor is more convenient, user friendly, and affordable than the other software packages in the market for personal use.

Education

The contribution to medical education is that students, researchers, and surgeons can interactively practice on anatomical structures and perceive their spatial position and 3D spatial relationships to each other, which allows them to comprehend anatomical structures much more efficiently. It can also be seen that the depiction of ELACs in anaglyph form, giving a sense of depth, shows 3D spatial relations better as well as contributing to the visualization,

Table 1. Total object volumes of the ethmoidal labyrinth air cells (ELACs)

ELACs on the right side		ELACs on the left side	
ELAC no.	Volume [mm ³]	ELAC no.	Volume [mm ³]
E1	109.18	E8	198.24
E2	35.929	E9	9.0503
E3	728.04	E10	340.72
E4	585.09	E11	338.94
E5	366.45	E12	445.58
E6	95.917	E13	472.92
E7	162.58	E14	205.47
Total	2083.19	E15	15.811
Mean	297.60	E16	16.401
		E17	20.446
		E18	133.47
		E19	174.41
		E20	236.74
		E21	79.716
		Total	2687.91
		Mean	191.99
Grand total volume: 4771.10			
Grand mean volume: 227.20			

perception, and interpretation. Moreover, VRML, a standard file format for representing 3D interactive views of anatomical structures, make it easy to send 3D anatomic models over the Internet by reducing the volume of data. Stereolithographic anatomical models provide an innovative and complementary tool for students, researchers, and surgeons to apprehend these anatomical structures tangibly.

DISCUSSION

One of the most ancient of sciences, anatomy has evolved over many centuries. Its methods have progressively encompassed dissection instruments, manual illustration, stains, microscopes, cameras and photography, and digital imaging systems. Like many other more modern scientific disciplines in the late 20th century, anatomy has also benefited from the revolutionary development of computers and their automated information management and analytical capabilities. By using newer methods of computer and information science, anatomists have made outstanding contributions to science, medicine, and education [37].

Several techniques are available to publish 3D models for readers. However, most require special devices such as stereoscopes and polarizing glasses. The anaglyph is one of the cheapest, and its images can be viewed with a red and a green/blue transparency in front of the reader's eyes. It can be used with all kinds of media and is easily produced on a PC using image processing software. The disadvantage of this method lies in the limited possibility of viewing coloured 3D models such as stereoblindness and in the considerable light loss experienced [14].

One of the main requirements of our medical image processing system is visualization functionality, where the user makes a 3D model and visualizes it. A browser-based solution for this purpose is the VRML standard [3], which is a Standard 3D world/object definition language designed for use in web applications [25]. There are many medical image processing software tools available for research and diagnosis purposes. However, most of these tools are available only as local applications. This limits the accessibility of the software to a specific machine, and thus the data and processing power of that application are not available to other workstations. Furthermore, there are operating system and processing power limitations which prevent such applications from running on every type of workstation. By developing web-based tools, it is possible for users to access the medical image processing functionalities wherever the Internet is available [25].

Another important aspect of medical image processing software is the extendibility of the software. As new processing algorithms are developed which are more robust, powerful, and suitable for specific applications, extensions of the software to include these algorithms are inevitable. Among these existing tools, most are not extendible. 3D Slicer is unique as it is open source and the user may add new processing routines to it. This feature has made this software more practical and appropriate for academic and research applications [25].

There are some fundamental advantages in using web-based medical software. Because of rapid changes in medical tools, the ability to update the software without interrupting the users or modifying their hardware and local software is necessary. Furthermore, there are many complex processing algorithms that require large memory and computational resources that may not be available on many client machines [10]. By centralizing processing power and using server machines with large computa-

tional resources, it is possible for the client machine to work as a simple terminal. The acquired data can be saved on the server side and users can access them via the network. The importance of this structure is particularly evident in emergency conditions where quick decisions should be made in locations where resources are limited, such as outside the hospital setting or in the field. Physicians can access and process the patient's medical data quickly and easily using the proposed web-base's medical imaging software [25].

Stereolithographic biomodelling, first described by Hull, is a rapidly developing technology that allows 3D imaging data to be used in the manufacture of accurate, solid plastic replicas of anatomical structures. Initially created for industry, stereolithography has been used to create 3D models for automotive design and engineering, part design and prototyping, and aerospace research [18]. The first reported use of stereolithographic biomodelling for replication of human anatomical structures was that of Mankovich et al. [26]. Currently, its application covers pre-operative planning of pelvic surgery [17], maxillofacial surgeries [6], temporal bone surgery [4], orbita surgery [24], vascular surgery [33], spinal surgery [27] and neurosurgery [34], endocrinology [21], cardiology [20], the fabrication of custom prosthetic devices [36], and the assessment of the degree of the bony and soft tissue injuries caused by trauma [13]. To our knowledge, this work is the first that dealt with stereolithographic biomodelling of ELACs. All imaging modalities display the ELACs as a whole. In our study, the ELACs were reconstructed separately and fabricated as solid models to reveal their spatial configurations and spatial relationships.

Comparing stereolithographic biomodels with milled 3D biomodels, the milling method shows shorter production time and lower costs. When complex or overhanging structures need to be rebuilt, however, stereolithography is judged to be the method of choice [32]. With stereolithographic casting it is possible to form very thinly tapered structures and to obtain more complex geometrical structures with smaller diameters. Many geometrical forms, which cannot be milled for technical reasons, can be produced using the stereolithography technique [41]. Stereolithography was found to be a superior technique as there were no limitations in producing hollow objects, highly complex anatomy was easily reproduced, and the plastic material was found to be durable and easily sterilized for intra-operative use [15].

It has enormous value as an educational teaching and patient information tool for obtaining consent for surgery. In a teaching hospital, stereolithographic biomodels form excellent education tool for teaching students the appreciation of the anatomy, pathology, surgical access, and techniques in reconstructive surgery. The stereolithographic biomodel can provide patients with extensive 3D information on the anatomy or pathology of the related structures [11].

The applications of stereolithographic biomodelling in reconstructive surgery have increased considerably in recent years to include diagnosis, surgical simulation, reconstructive planning, and patient information. The main advantages are reduction of surgical time and morbidity of the patients as well as improvement in the quality of the surgical results [11]. Decreased exposure time to general anaesthesia, decreased blood loss, and lessened wound exposure time are all significant patient benefits from reduced operating time [22]. Simulation surgery can be performed on the stereolithographic biomodel to check its feasibility and to predict the surgical outcome [11].

Development of the technique has been facilitated by improvements in medical imaging technology, computer hardware, 3D image processing software, and the technology transfer of engineering methods into the field of medicine [39]. The accuracy of stereolithographic models is influenced by factors in each step of the process: data acquisition, 3D data rendering, data transfer, model fabrication, post-fabrication changes, and handling [9]. Depending on the sudden appearance and disappearance of the anatomical structures in pertinent cryosections, flattenings were seen where reconstructions began and ended in our study. The ELACs' ducts or orifices could not be distinguished at this cryosectional resolution.

The volume of the air cavities in the paranasal sinuses is not only the simplest, but also the most significant parameter for their evaluation. The ethmoid sinus always exists at birth. The anterior ethmoid sinus develops earlier than the posterior ethmoid sinus. Development of the ethmoid sinus continues until early teenage years. The ethmoid sinus reaches adult dimensions between 12 and 13 years of age [28]. Wolf found that by 10 years of age, the ethmoid sinus has almost reached adult proportions [40]. Lee et al. [23] reported that there was no change in the volume in the ethmoid sinus after 10–12 years of age, and endoscopic sinus surgery might change

the facial growth of children < 10–12 years of age. Park et al. [28] reported that development of the ethmoid sinus showed a fast phase between birth and 7 years of age. There were no statistically significant changes in volume of the ethmoid sinus after 9 years of age. The mean volume of the ethmoid sinus at birth was $0.41 \pm 0.08 \text{ cm}^3$. The ethmoid sinuses rapidly increased until 7 years of age, were completed by 15–16 years of age, and the mean volume after full growth was $4.51 \pm 0.92 \text{ cm}^3$. In our study, the total volume of the ELACs using the Surfdriver software was calculated to be 4.77 cm^3 . The total volume of the ELACs measured with the volumetric measuring tool of the software is consistent with those reported in previous studies, a fact which supports the accuracy and reliability of our measurement method.

In conclusion, this is the first study in the literature describing the 3D structure of the ELACs and presenting their 3D solid model using a stereolithographic biomodelling technique. The combination of Surfdriver and 3D-Doctor software could be effectively used for the manufacture of 3D solid models from serial sections. The reproduction of the ELACs by stereolithography is reliable enough to be used for preoperative evaluation, for surgical planning, and for anatomy teaching. Moreover, the representation of the ELACs in anaglyph form can provide benefits in terms of visualization, perception, and interpretation. The VRML file format enables 3D models to be transferred over the Internet.

In the near future, advances in rapid prototyping techniques will enable replicas of complicated anatomical structures to be manufactured rapidly and at low cost; and improvements in the stereolithographic technique will allow the production of dynamic models instead of nonfunctional static models. Additionally, the advent of new biomodel material compositions in the future will allow the limitations concerning material properties to be overcome and more realistic solid biomodels to be obtained.

REFERENCES

- Ackerman MJ, Banvard RA (2000) Imaging outcomes from The National Library of Medicine's Visible Human Project. *Comput Med Imaging Graph*, 24: 125–126.
- Alan M, Mavroidis C, Langrana N, Bidaud P (1999) Mechanism design using rapid prototyping. Tenth World Congress on the theory of machines and mechanisms. Oulu, Finland: Oulu University Press, 930–938.
- Ames AL, Nadeau DR, J.L. Moreland JL (1997) VRML 2.0 Sourcebook, Second edition, John Wiley & Sons, Inc.
- Bakhos D, Velut S, Robier A, Al Zahrani M, Lescanne E (2010) Three-dimensional modeling of the temporal bone for surgical training. *Otol Neurotol*, 31: 328–334.
- Barry CJ, Kanagasingam Y, Morgan W (1999) Optic disc topographic changes post-trabeculectomy visualized by anaglyphs. *Aust NZJ Ophthalmol*, 27: 79–83.
- Bell RB (2010) Computer planning and intraoperative navigation in cranio-maxillofacial surgery. *Oral Maxillofac Surg Clin North Am*, 22: 135–156.
- Beylot P, Gingins P, Kalra P, Thalmann NM, Maurel W, Thalmann D, Fasel J (1996) 3D Interactive topological modeling using visible human dataset. *Com Graph Forum*, 15: 33–34.
- Bro-Nielsen M (1997) Rigid registration of CT, MR and cryosection images using a GLCM framework. In: *CVRMed/MRCAS'97*. Springer Verlag, France, pp. 171–180.
- Chang PS, Parker TH, Patrick CW, Miller MJ (2003) The accuracy of stereolithography in planning craniofacial bone replacement. *J Craniofac Surg*, 14: 164–170.
- Chen HM, Lin YC (2008) Web-FEM: an internet-based finite-element analysis framework with 3D graphics and parallel computing environment. *Adv Eng Softw*, 39: 55–68.
- Cheung LK, Wong MCM, Wong LLS (2001) The applications of stereolithography in facial reconstructive surgery. Medical imaging and augmented reality: First International Workshop; 2001 June 10–12; MIAR, Hong Kong, China: IEEE Computer Society; pp. 10–15.
- Decraemer WF, Dirckx JJ, Funnell WRJ (2003) Three-dimensional modeling of the middle-ear ossicular chain using a commercial high-resolution X-Ray CT scanner. *J Assoc Res Otolaryngol*, 4: 250–263.
- Dolz MS, Cina SJ, Smith R (2000) Stereolithography: a potential new tool in forensic medicine. *Am J Forensic Med Pathol*, 21: 119–123.
- Doneus M, Hanke K (1999) Anaglyph images-still a good way to look at 3D objects? URL: <http://cipa.icomos.org/text%20files/olinda/99c411.pdf> [accessed November 2010].
- D'Urso PS, Earwaker WJ, Barker TM, Redmond MJ, Thompson RG, Effeney DJ, Tomlinson FH (2000) Custom cranioplasty using stereolithography and acrylic. *Br J Plas Surg*, 53: 200–204.
- Hastings-Trew J (2010) Cinema 4D Global Illumination. URL: <http://planetpixlemporium.com/tutorialpages/global.html> [accessed October 2010].
- Holubar SD, Hassinger JP, Dozois EJ, Camp JC, Farley DR, Fidler JL, Pawlina W, Robb RA (2009) Virtual pelvic anatomy and surgery simulator: an innovative tool for teaching pelvic surgical anatomy. *Stud Health Technol Inform*, 142: 122–124.
- Jacobs PF (1992) Rapid prototyping and manufacturing: fundamentals of stereolithography. McGraw-Hill, New York, pp. 5–7.
- Jacobs PF (1996) Stereolithography and other RP&M technologies. ASME Press, New York, pp. 5–10.
- Jacobs S, Grunert R, Mohr FW, Falk V (2008) 3D-imaging of cardiac structures using 3D heart models for planning in heart surgery: a preliminary study. *Interact Cardiovasc Thorac Surg*, 7: 6–9.

21. Kapakin S, Demiryurek D (2009) The reproduction accuracy for stereolithographic model of the thyroid gland derived from the visible human dataset. *Saudi Med J*, 30: 887–892.
22. Kernan BT, Wimsatt JA 3rd. (2000) Use of a stereolithography model for accurate, preoperative adaptation of a reconstruction plate. *J Oral Maxillofac Surg*, 58: 349–351.
23. Lee CH, Rhee CS, Oh SJ, Jung YH, Min YG, Kim IO (2000) Development of the paranasal sinuses in children: MRI study. *Korean J. Otolaryngol*, 43: 507–513.
24. Lieger O, Richards R, Liu M, Lloyd T (2010) Computer-assisted design and manufacture of implants in the late reconstruction of extensive orbital fractures. *Arch Facial Plast Surg*, 12: 186–191.
25. Mahmoudi SE, Akhondi-Asl A, Rahmani R, Faghih-Roohi S, Taimouri V, Sabouri A, Soltanian-Zadeh H (2010) Web-based interactive 2D/3D medical image processing and visualization software. *Comput Methods Programs Biomed*, 98: 172–182.
26. Mankovich NJ, Cheeseman AM, Stoker NG (1990) The display of three-dimensional anatomy with stereolithographic models. *J Digit Imaging*, 3: 200–203.
27. Paiva WS, Amorim R, Bezerra DA, Masini M (2007) Application of the stereolithography technique in complex spine surgery. *Arq Neuropsiquiatr*, 65: 443–445.
28. Park IH, Song JS, Choi H, Kim TH, Hoon S, Lee SH, Lee HM (2010) Volumetric study in the development of paranasal sinuses by CT imaging in Asian: a pilot study. *Int J Pediatr Otorhinolaryngol*, 74: 1347–1350.
29. Purnell MA (2003) Casting, replication, and anaglyph stereo imaging of microscopic detail in fossils, with examples from conodonts and other jawless vertebrates. *Palaeontol Electron*, 6: 1–11.
30. Robb RA ed. (1990) A software system for interactive and quantitative analysis of biomedical images. In *3D imaging in medicine*. Springer Verlag, Berlin, pp. 333–361.
31. Robb RA (2000) Three-dimensional visualization in medicine and biology. In: Bankman IN ed. *Handbook of medical imaging: processing and analysis*. Academic Press, San Diego, pp. 685–712.
32. Santler G, Kärcher H, Kern R (1998) Stereolithography models vs. milled 3D models. Production, indications, accuracy. *Mund Kiefer Gesichtschir*, 2: 91–95.
33. Sodiano R, Schmauss D, Schmitz C, Bigdeli A, Haeberle S, Schmoeckel M, Markert M, Lueth T, Freudenthal F, Reichart B, Kozlik-Feldmann R (2009) 3-dimensional printing of models to create custom-made devices for coil embolization of an anastomotic leak after aortic arch replacement. *Ann Thorac Surg*, 88: 974–978.
34. Solaro P, Pierangeli E, Pizzoni C, Boffi P, Scalese G (2008) From computerized tomography data processing to rapid manufacturing of custom-made prostheses for cranioplasty. Case report. *J Neurosurg Sci*, 52: 113–116.
35. Spitzer V, Ackerman MJ, Scherzinger AL, Whitlock D (1996) The visible human male: A technical report. *JAMA*, 3: 118–130.
36. Staffa G, Nataloni A, Compagnone C, Servadei F (2007) Custom made cranioplasty prostheses in porous hydroxyapatite using 3D design techniques: 7 years experience in 25 patients. *Acta Neurochir (Wien)*, 149: 161–170.
37. Trelease RB (2002) Anatomical informatics: millennial perspectives on a newer frontier. *Anat Rec*, 269: 224–235.
38. Warrick PA, Funnell WR (1998) A VRML-based anatomical visualization tool for medical education. *IEEE Trans Inf Technol Biomed*, 2: 55–61.
39. Winder J, Bibb R (2005) Medical rapid prototyping technologies: state of the art and current limitations for application in oral and maxillofacial surgery. *J Oral Maxillofac Surg*, 63: 1006–1015.
40. Wolf G, Anderhuber W, Kuhn F (1993) Development of the paranasal sinuses in children: implications for paranasal sinus surgery. *Ann Otol Rhinol Laryngol*, 102: 705–711.
41. Wurm G, Tomancok B, Pogady P, Holl K, Trenkler J (2004) Cerebrovascular stereolithographic biomodeling for aneurysm surgery. Technical notes. *J Neurosurg*, 100: 139–145.
42. Wurm G, Tomancok B, Holl K, Trenkler J (2004) Prospective study on cranioplasty with individual carbon fiber reinforced polymer (CFRP) implants produced by means of stereolithography. *Surg Neurol*, 62: 510–521.